JOURNAL OF ENZYME INHIBITION AND MEDICINAL CHEMISTRY
2025, VOL. 40, NO. 1, 2470310
https://doi.org/10.1080/14756366.2025.2470310

Taylor & Francis
Taylor & Francis Group

RESEARCH ARTICLE

OPEN ACCESS Check for updates

# Synthesis and evaluation of 5, 6-dihydro-8*H*-isoquinolino[1, 2-*b*]quinazolin-8-one derivatives as novel non-lipogenic ABCA1 up-regulators with inhibitory effects on macrophage-derived foam cell formation

Changhuan Yang, Lin Chen, Yanmei Jiang, Demeng Sun and Yun Hu

School of Bioengineering, Zunyi Medical University, Zhuhai, China

**ABSTRACT**

Increasing the expression of ATP-binding cassette transporter A1 (ABCA1) can lower cellular cholesterol levels and prevent foam cell formation. In this study, a series of 5, 6-dihydro-8*H*-isoquinolino[1, 2-*b*] quinazolin-8-one derivatives were synthesised and assessed for their ability to up-regulate ABCA1 expression. The structure-activity relationship was explored and summarised. Among the 28 derivatives, compound **3** exhibited the most potent activity in activating the ABCA1 promoter (2.50-fold), significantly up-regulating both ABCA1 mRNA and protein levels in RAW264.7 macrophage cells. Mechanism studies revealed that compound **3** acted by targeting the LXR-involved pathway. In a foam cell model, compound **3** reduced ox-LDL-induced lipid accumulation and thereby inhibited foam cell formation. Moreover, compared to the LXR agonist T0901317, compound **3** led to minimal accumulation of unwanted lipids and triglycerides in HepG2 cells. With little cytotoxicity towards all the tested cell lines, compound **3** holds promise as a novel potential anti-atherogenic agent for further exploration.

**ARTICLE HISTORY**
Received 26 October 2024
Revised 5 February 2025
Accepted 10 February 2025

**KEYWORDS**
ABCA1; macrophage foam cell; atherosclerosis; quinazolinone

## Introduction

Atherosclerosis is a chronic inflammatory, immune, and epigenetic disease of the arterial walls, which is the main cause of cardiovascular events such as unstable angina pectoris, myocardial infarction, ischaemic stroke, and sudden cardiovascular death[1]. The commonly used drugs of statins could only reduce the incidence of cardiovascular events by about one third[2,3]. Thus, development of novel agents with improved therapeutic benefits has always received much attention.

The pathological basis of atherosclerosis is the formation of atherosclerotic plaques in the arterial wall that contain a large number of necrotic cells and inflammatory cells[4]. In the pathogenic development, one of the key factors that driving the formation of atherosclerotic plaques is the macrophage foam cells, which is considered as a promising target for therapeutic intervention in atherosclerosis[5,6]. The formation of macrophage foam cells is attributed to the intracellular accumulation of cholesterol esters (CE)[7]. In the early stage of atherosclerosis, excess free cholesterol is released in modified LDL-loaded macrophages and undergoes re-esterification in the endoplasmic reticulum[8]. However, intracellular cholesterol efflux is insufficient, ultimately resulting in the formation of foam cells stuffed with lipid droplets[1,9]. Therefore, promoting cholesterol efflux could reduce the intracellular cholesterol level and inhibit foam cell formation.

One of the main cholesterol transporters for cholesterol efflux is ATP-binding cassette transporter A1 (ABCA1). ABCA1 is a member of the ABC transporter superfamily that utilises ATP as a source of energy to transport various lipids across cellular membranes[10]. With the help of ABCA1, the removed cholesterol from macrophage foam cells undergoes the so-called reverse cholesterol transport (RCT) process, during which the cholesterol is transported to apolipoproteins to form high-density lipoproteins (HDL), which is then returned to the liver for excretion in the bile and ultimately in the feces[11,12]. Thus, ABCA1 is critical for maintaining cholesterol homeostasis in the human body. Evidence shows that the lack of ABCA1 would cause severe HDL deficiency and a much higher risk of cardiovascular disease, while overexpression of ABCA1 in macrophages promotes RCT and protects against atherosclerosis[13]. From this perspective, therapeutic agents that elevates the expression of ABCA1 would exert beneficial effects to atherosclerosis treatment.

In general, ABCA1 expression is transcriptionally regulated by nuclear receptors including liver X receptor (LXR), retinoid X receptor (RXR), and peroxisome proliferator-activated receptor (PPAR)[14,15]. Among them, LXR has been extensively investigated. Several lines of synthetic LXR agonists including hexafluoroisopropanol derivatives (e.g. T0901317), tertiary amine carboxylic acid derivatives (e.g. GW3965), pyrazole derivatives (e.g. LXR-623) and quinoline carboxylic acid derivatives (e.g. WAY254011) etc. have been developed (Figure 1(A))[16,17]. However, most of these agonists cannot be used clinically despite their ability to upregulate ABCA1 expression, due to undesirable side effects such as hepatic steatosis and hypertriglyceridaemia, which are induced by their upregulation of sterol regulatory element-binding protein 1c (SREBP-1c) and fatty acid synthase (FAS) in the liver[18,19]. Consequently, there is a pressing

**CONTACT** Yun Hu ce04hy@mail2.sysu.edu.cn School of Bioengineering, Zunyi Medical University, Zhuhai Campus, Zhuhai 519041, China

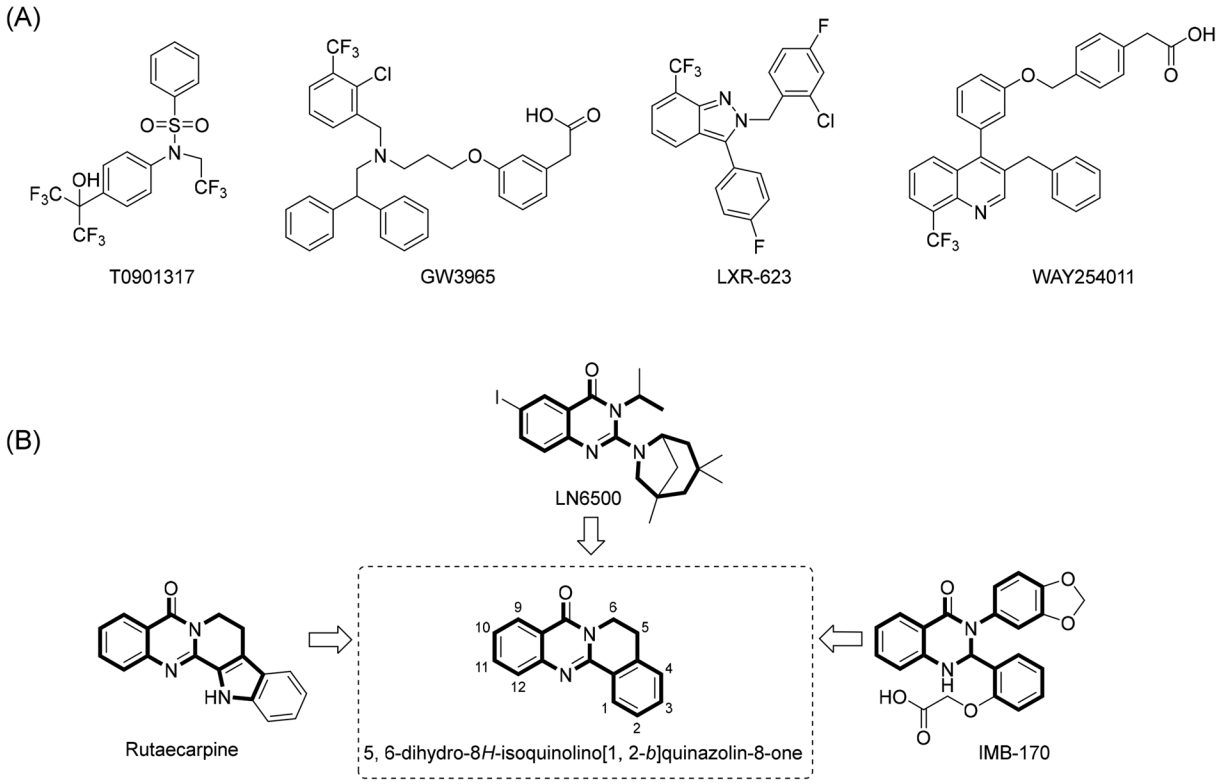


**Figure 1.** (A) The chemical structure of LXR agonist T0901317; (B) The chemical structures of quinazolinone-containing compounds with ABCA1 up-regulating activity and the chemical structure of 5, 6-dihydro-8*H*-isoquinolino[1, 2-*b*]quinazolin-8-one in the present study.

need to discover novel ABCA1 up-regulators without inducing lipogenesis[20].

In previous studies, several quinazolinone compounds with ABCA1 up-regulating activity were discovered (Figure 1(B)). Rutaecarpine, a natural indole alkaloid isolated from Tetradium ruticarpum, was identified as a potent ABCA1 up-regulator with a maximum up-regulating value of 240% in ABCA1p-LUC HepG2 cells[21]. The synthetic quinazolinone derivatives LN6500 and IMB-170 were also found to increase the expression of ABCA1 in macrophage cells[22]. These compounds share a common quinazolinone scaffold and exhibit similar chemical structures in terms of molecular length or shape. Thus, we hypothesise that the quinazolinone structure could serve as a privileged scaffold for the rational design of novel ABCA1 up-regulators.

Inspired by the structure similarity with the above active quinazolinone compounds, in the present study we synthesised a series of derivatives of a polycyclic fused quinazolinone, 5, 6-dihydro-8*H*-isoquinolino[1, 2-*b*]quinazolin-8-one (Figure 1(B)), and screened for the activity of up-regulating ABCA1 expression using an ABCA1-promoter reporter gene assay. The structure-activity relationship (SAR) of these compounds was explored and summarised. The potent compound is further evaluated for the inhibitory effect on the formation of macrophage foam cells. Besides, the side effect of the hit compound on inducing hepatic lipogenesis is investigated as well.

## Materials and methods

### *General methods*

The isatins, 1, 2, 3, 4-tetrahydroisoquinoline, benzaldehyde and 2-aminobenzamide were purchased from Bide Pharmatech Ltd (Shanghai, China). The Dulbecco's Modified Eagle's Medium (DMEM) and foetal bovine serum (FBS) was purchased from Gibco (USA). Mouse-derived macrophage RAW264.7, human cervical cancer cell Hela and human hepatocellular carcinoma cell HepG2 were obtained from the Typical Culture Collection Centre of China. The Human oxidised low density lipoprotein (ox-LDL) and DiI-ox-LDL (ox-LDL labelled with 1,1′-dioctadecyl-3,3,3′,3′-tetramethylindocarbocyanine perchlorate) were purchased from Yiyuan Biotechnologies (GuangZhou, China). The rabbit polyclonal ABCA1 antibody was obtained from Novus Biological Inc. (USA). The anti-β-actin antibody and the secondary antibodies (anti-rabbit and anti-mouse IgG-HRP) were obtained from Santa Cruz Biotech Corp (USA). Other reagents and solvents were commercially available and used without additional purification. Thin layer chromatography (TLC) was conducted on glass plates coated with silica gel containing a fluorescent indicator ($GF_{254}$). Column chromatography utilised silica gel with a mesh size of 200–300. The $^{1}H$ NMR and $^{13}C$ NMR spectra were recorded using TMS as an internal standard on a Bruker BioSpin Ultra shield NMR system. The purity of compounds intended for biological evaluation was assessed using either a Waters Ultimate High Performance Liquid Chromatography (HPLC) system with UV detection at 200–400 nm or a Shimadzu HPLC system with UV detection at 254 or 365 nm.

The compounds were eluted on UPLC with acetonitrile/water (0.1% formic acid, v/v) in ratios of 20:80–75:25 at a flow rate of 0.2 ml/min or eluted on HPLC with methyl/water (1/1, v/v)/water (0.1% formic acid, v/v) in ratios of 50:30 at a flow rate of 0.4 ml/min. The purities of compounds were calculated as the percentage peak area of the analysed compound, and retention times ($t_R$) were presented in minutes. High resolution mass spectra (HRMS) were recorded on Agilent Technologies 6530 Q-TOF.

### *General procedure for the synthesis of compounds 1–18, 23, 25–27*

Compounds **1–18**, **23**, **25–27** were synthesised as previously described[23]. 2 mmol isatin (**a**) and 2 mmol corresponding tetrahydroisoquinoline (**b**) were dissolved in 4 ml DMSO. Then 6 mmol tert-Butyl hydroperoxide (TBHP) was added. The mixture was vigorously stirred at 120 °C for 12–15 h and the reaction was monitored by TLC until completed. After cooling to room temperature, the reaction mixture was extracted with ethyl acetate. The organic phase was combined and dried over anhydrous magnesium sulphate. Then the ethyl acetate was collected and concentrated *in vacuo*. The crude product was purified by chromatography column with ethyl acetate/petroleum ether or recrystallization with ethanol.

*5, 6-dihydro-8H-isoquinolino[1, 2-b]quinazolin-8-one* (**1**) Yield 1.78%. UPLC purity 97.83%, $t_R$=3.528 min。$^1$H NMR (400 MHz, DMSO-$d_6$) δ 8.37 (d, *J*=7.8 Hz, 1H), 8.17 (d, *J*=7.9 Hz, 1H), 7.83 (t, *J*=7.7 Hz, 1H), 7.74 (d, *J*=8.1 Hz, 1H), 7.53 (dt, *J*=10.0, 7.4 Hz, 2H), 7.46 (t, *J*=7.5 Hz, 1H), 7.41 (d, *J*=7.5 Hz, 1H), 4.30 (t, *J*=6.5 Hz, 2H), 3.11 (t, *J*=6.5 Hz, 2H).$^{13}$C NMR (101 MHz, DMSO-$d_6$) δ 161.05, 149.72, 147.74, 138.17, 134.82, 132.20, 129.52, 128.23, 127.83, 127.75, 127.64, 126.96, 126.75, 120.84, 39.69, 26.87. HRMS calcd for $C_{16}H_{12}N_2O$ [M+H]$^+$: 249.1028, m/z found: 249.0856.

*9-chloro-5, 6-dihydro-8H-isoquinolino[1, 2-b]quinazolin-8-one* (**2**) Yield 5.85%, HPLC purity 98.68%, $t_R$=9.726 min。$^1$H NMR (400 MHz, DMSO-$d_6$) δ 8.34 (d, J=7.8 Hz, 1H), 7.72 (d, J=7.8 Hz, 1H), 7.67 (d, J=7.7 Hz, 1H), 7.53 (dd, J=12.9, 7.6 Hz, 2H), 7.46 (d, J=7.4 Hz, 1H), 7.41 (d, J=7.2 Hz, 1H), 4.23 (t, J=6.4 Hz, 2H), 3.10 (t, J=6.6 Hz, 2H).$^{13}$C NMR (101 MHz, DMSO-$d_6$) δ 159.13, 150.39, 150.24, 138.35, 134.53, 133.06, 132.51, 129.25, 129.08, 128.24, 127.82, 127.65, 127.36, 117.77, 39.74, 26.79.

*9-bromo-5, 6-dihydro-8H-isoquinolino[1, 2-b]quinazolin-8-one* (**3**) Yield 3.34%. UPLC purity 97.60%, $t_R$=3.528 min。$^1$H NMR (400 MHz, DMSO-$d_6$) δ 8.34 (d, *J*=7.6 Hz, 1H), 7.73 (t, *J*=7.3 Hz, 2H), 7.66−7.63 (m, 1H), 7.56 (t, *J*=7.0 Hz, 1H), 7.46 (t, *J*=7.5 Hz, 1H), 7.42 (d, *J*=7.4 Hz, 1H), 4.23 (t, *J*=6.5 Hz, 2H), 3.12 (t, *J*=6.5 Hz, 2H). $^{13}$C NMR (101 MHz, DMSO-$d_6$) δ 159.25, 150.19, 150.15, 138.36, 134.91, 133.05, 132.54, 129.11, 128.27, 128.06, 127.79, 127.67, 120.89, 118.71, 26.78. HRMS calcd for $C_{16}H_{11}BrN_2O$ [M+H]$^+$: 327.0133, m/z found: 327.0150.

*9-methyl-5, 6-dihydro-8H-isoquinolino[1, 2-b]quinazolin-8-one* (**4**) Yield 1.57%, HPLC purity 98.77%, $t_R$=18.767 min。$^1$H NMR (600 MHz, DMSO-$d_6$) δ 8.34 (d, *J*=7.8 Hz, 1H), 8.21 (d, *J*=8.6 Hz, 1H), 7.55 (t, *J*=7.4 Hz, 1H), 7.46 (t, *J*=7.6 Hz, 1H), 7.41 (d, *J*=7.5 Hz, 1H), 7.34 (d, *J*=8.6 Hz, 1H), 4.25 (t, *J*=6.5 Hz, 2H), 3.11 (t, *J*=6.5 Hz, 2H), 3.01 (s, 3H). $^{13}$C NMR (151 MHz, DMSO-$d_6$) δ 160.76, 150.07, 149.27, 144.32, 142.57, 138.25, 132.41, 129.17, 128.26, 127.81, 127.75, 127.68, 120.42, 101.92, 27.93, 26.89.

*10-fluoro-5, 6-dihydro-8H-isoquinolino[1, 2-b]quinazolin-8-one* (**5**) Yield 10.2%, HPLC purity 99.93%, $t_R$=11.714 min。$^1$H NMR (400 MHz, DMSO-$d_6$) δ 8.35 (d, *J*=7.7 Hz, 1H), 7.87–7.76 (m, 2H), 7.72 (t, *J*=8.5 Hz, 1H), 7.55 (t, *J*=7.3 Hz, 1H), 7.49–7.38 (m, 2H), 4.30 (t, *J*=6.0 Hz, 2H), 3.12 (t, *J*=5.8 Hz, 2H). $^{13}$C NMR (101 MHz, DMSO-$d_6$) δ 161.63, 160.50, 160.47, 159.19, 149.32, 149.30, 144.69, 138.12, 132.26, 130.67, 130.59, 129.36, 128.26, 127.78, 127.68, 123.53, 123.29, 122.04, 121.95, 111.42, 111.19, 26.80.

*10-chloro-5, 6-dihydro-8H-isoquinolino[1, 2-b]quinazolin-8-one* (**6**) Yield 5.97%, HPLC purity 97.46%, $t_R$=11.694 min。$^1$H NMR (400 MHz, DMSO-$d_6$) δ 8.34–8.29 (m, 1H), 8.02 (s, 1H), 7.75 (dt, *J*=40.5, 7.1 Hz, 2H), 7.54–7.50 (m, 1H), 7.41 (dt, *J*=22.5, 6.9 Hz, 2H), 4.28–4.24 (m, 2H), 3.11–3.07 (m, 2H). $^{13}$C NMR (101 MHz, DMSO-$d_6$) δ 160.08, 150.13, 146.44, 138.14, 134.86, 132.38, 131.08, 129.92, 129.19, 128.22, 127.87, 127.64, 125.63, 121.93, 39.97, 26.73.

*10-bromo-5, 6-dihydro-8H-isoquinolino[1, 2-b]quinazolin-8-one* (**7**) Yield 8.98%, HPLC purity 98.75%, $t_R$=12.471 min。$^1$H NMR (400 MHz, DMSO-$d_6$) δ 8.32 (d, *J*=7.8 Hz, 1H), 8.19 (s, 1H), 7.93 (d, *J*=8.7 Hz, 1H), 7.64 (d, *J*=8.7 Hz, 1H), 7.54 (t, *J*=7.5 Hz, 1H), 7.46–7.38 (m, 2H), 4.26 (t, *J*=6.7 Hz, 2H), 3.10 (t, *J*=6.7 Hz, 2H). $^{13}$C NMR (101 MHz, DMSO-$d_6$) δ 159.99, 150.27, 146.73, 138.21, 137.62, 132.44, 130.10, 129.23, 128.78, 128.26, 127.91, 127.68, 122.34, 119.24, 39.89, 26.73.

*10-methyl-5, 6-dihydro-8H-isoquinolino[1, 2-b]quinazolin-8-one* (**8**) Yield 8.3%, HPLC purity 99.37%, $t_R$=10.727 min。$^1$H NMR (400 MHz, DMSO-$d_6$) δ 8.41–8.32 (m, 1H), 7.97 (s, 1H), 7.65 (s, 2H), 7.59–7.35 (m, 3H), 4.29 (s, 2H), 3.11 (s, 2H), 2.47 (s, 3H). $^{13}$C NMR (101 MHz, DMSO-$d_6$) δ 160.97, 148.99, 145.79, 138.04, 136.73, 136.18, 132.04, 129.62, 128.23, 127.70, 127.67, 127.63, 126.08, 120.61, 39.70, 26.95, 21.36.

*10-methoxy-5, 6-dihydro-8H-isoquinolino[1, 2-b]quinazolin-8-one* (**9**) Yield 10.72%, HPLC purity 96.31%, $t_R$=8.837 min。$^1$H NMR (400 MHz, DMSO-$d_6$) δ 8.33 (d, *J*=7.6 Hz, 1H), 7.69 (d, *J*=8.9 Hz, 1H), 7.54–7.50 (m, 2H), 7.46–7.39 (m, 3H), 4.30 (t, *J*=6.5 Hz, 2H), 3.11 (t, *J*=6.5 Hz, 2H). $^{13}$C NMR (101 MHz, DMSO-$d_6$) δ 160.77, 158.20, 147.69, 142.28, 137.79, 131.81, 129.66, 129.54, 128.21, 127.62, 127.51, 124.43, 121.65, 106.75, 56.14, 26.97.

*11-chloro-5, 6-dihydro-8H-isoquinolino[1, 2-b]quinazolin-8-one* (**10**) Yield 11.27%, HPLC purity 97.89%, $t_R$=12.445 min。$^1$H NMR (400 MHz, DMSO-$d_6$) δ 8.34 (d, *J*=7.7 Hz, 1H), 8.13 (d, *J*=8.5 Hz, 1H), 7.76 (s, 1H), 7.62–7.50 (m, 2H), 7.46 (t, *J*=7.4 Hz, 1H), 7.41 (d, *J*=7.3 Hz, 1H), 4.27 (t, *J*=6.2 Hz, 2H), 3.11 (t, *J*=6.0 Hz, 2H). $^{13}$C NMR (101 MHz, DMSO-$d_6$) δ 160.54, 151.11, 148.86, 139.41, 138.34, 132.57, 129.20, 128.83, 128.28, 128.00, 127.69, 127.15, 126.76, 119.63, 39.76, 26.73.

*11-bromo-5, 6-dihydro-8H-isoquinolino[1, 2-b]quinazolin-8-one* (**11**) Yield 8.18%, HPLC purity 97.89%, $t_R$=12.445 min。$^1$H NMR (400 MHz, DMSO-$d_6$) δ 8.44 (d, *J*=7.7 Hz, 1H), 8.13 (t, *J*=8.0 Hz, 2H), 7.55 (t, *J*=7.0 Hz, 1H), 7.50–7.48 (m, 1H), 7.40 (d, *J*=7.2 Hz, 2H), 4.31–4.28 (m, 2H), 3.18–3.12 (m, 2H). $^{13}$C NMR (101 MHz, DMSO-$d_6$) δ 160.65, 150.51, 138.24, 138.06, 132.57, 129.35, 128.24, 128.17, 127.70, 127.58, 126.59, 122.42, 26.71.

*11-methoxy-5, 6-dihydro-8H-isoquinolino[1, 2-b]quinazolin-8-one* (**12**) Yield 5.73%, HPLC purity 99.89%, $t_R$=8.361 min。$^1$H NMR (400 MHz, DMSO-$d_6$) δ 8.35 (d, *J*=7.5 Hz, 1H), 8.04 (d, *J*=8.7 Hz, 1H), 7.55–7.52 (m, 1H), 7.49–7.34 (m, 2H), 7.15 (s, 1H), 7.07 (d, *J*=8.4 Hz, 1H), 4.25 (t, 2H), 3.92 (s, 3H), 3.10 (t, 2H). $^{13}$C NMR (101 MHz, DMSO-$d_6$) δ 164.46, 160.55, 150.25, 149.93, 138.18, 132.19, 129.53, 128.34, 128.23, 127.80, 127.59, 116.72, 114.38, 108.58, 56.16, 26.93.

*12-chloro-5, 6-dihydro-8H-isoquinolino[1, 2-b]quinazolin-8-one* (**13**) Yield 10.86%, HPLC purity 99.04%, $t_R$=10.861 min。$^1$H NMR (400 MHz, DMSO-$d_6$) δ 8.42 (s, 1H), 8.11 (s, 1H), 7.97 (s, 1H), 7.56–7.42 (m, 4H), 4.29 (s, 2H), 3.13 (s, 2H). $^{13}$C NMR (101 MHz, DMSO-$d_6$) δ 160.61, 150.39, 144.22, 138.24, 134.75, 132.55, 131.20, 129.32, 128.22, 128.11, 127.69, 127.10, 125.88, 122.48, 26.66.

*12–fluoro-5, 6-dihydro-8H-isoquinolino[1, 2-b]quinazolin-8-one* (**14**) Yield 16.17%, UPLC purity 98.86%, $t_R$=2.766 min。$^1$H NMR (400 MHz, DMSO-$d_6$) δ 8.34 (d, *J*=7.8 Hz, 1H), 7.94 (d, *J*=8.0 Hz, 1H), 7.71–7.60 (m, 1H), 7.55 (t, *J*=7.3 Hz, 1H), 7.50–7.44 (m, 2H), 7.40 (d, *J*=7.5 Hz, 1H), 4.29 (t, *J*=6.5 Hz, 2H), 3.12 (t, *J*=6.5 Hz, 2H). $^{13}$C NMR (101 MHz, DMSO-$d_6$) δ 160.23, 158.19, 155.67, 150.27, 138.22, 137.24, 137.13, 132.49, 129.31, 128.22, 128.01, 127.71, 127.09, 127.02, 122.81, 122.50, 122.46, 120.13, 119.94, 39.83, 26.70. calcd for $C_{16}H_{11}FN_2O$: 266.0855, m/z [M+H]$^+$ found: 267.0796.

*12-methyl-5, 6-dihydro-8H-isoquinolino[1, 2-b]quinazolin-8-one* (**15**) Yield 6.45%, HPLC purity 99.28%, $t_R$=12.081 min。$^1$H NMR (400 MHz, DMSO-$d_6$) δ 8.41 (d, *J*=7.6 Hz, 1H), 7.98 (d, *J*=7.8 Hz, 1H), 7.66 (d, *J*=6.9 Hz, 1H), 7.55–7.51 (m, 1H), 7.48–7.44 (m, 1H), 7.40–7.36 (m, 2H), 4.28 (t, *J*=6.6 Hz, 2H), 3.10 (t, *J*=6.6 Hz, 2H), 2.63 (s, 3H). $^{13}$C NMR (101 MHz, DMSO-$d_6$) δ 161.28, 148.58, 146.12, 138.03, 135.80, 135.01, 132.08, 129.81, 128.19, 127.87, 127.64, 126.46, 124.40, 120.73, 26.87, 17.37.

*12-(trifluoromethyl)-5, 6-dihydro-8H-isoquinolino[1, 2-b] quinazolin-8-one* (**16**) Yield 6.83%, HPLC purity 99.61%, $t_R$=10.544 min。$^1$H NMR (400 MHz, DMSO-$d_6$) δ 8.41 (d, $J$=8.0 Hz, 1H), 8.36 (d, $J$=8.0 Hz, 1H), 8.19 (d, $J$=7.5 Hz, 1H), 7.64–7.56 (m, 2H), 7.50 (t, $J$=7.6 Hz, 1H), 7.42 (d, $J$=7.5 Hz, 1H), 4.31 (t, $J$=6.6 Hz, 2H), 3.14 (t, $J$=6.6 Hz, 2H). $^{13}$C NMR (101 MHz, DMSO-$d_6$) δ 160.41, 150.74, 145.22, 138.50, 132.81, 132.51, 132.46, 132.41, 132.36, 131.44, 129.18, 128.29, 128.10, 127.80, 126.07, 125.65, 125.35, 125.06, 122.93, 122.02, 26.56.

*10, 12-dimethyl-5, 6-dihydro-8H-isoquinolino[1, 2-b]quinazolin-8-one* (**17**) Yield 1.95%. UPLC purity 98.97%, $t_R$=4.416 min。$^1$H NMR (400 MHz, DMSO-$d_6$) δ 8.38 (d, $J$=7.8 Hz, 1H), 7.77 (s, 1H), 7.50–7.39 (m, 4H), 4.27 (t, $J$=6.4 Hz, 2H), 3.09 (t, $J$=6.4 Hz, 2H), 2.59 (s, 3H), 2.40 (s, 3H). $^{13}$C NMR (101 MHz, DMSO-$d_6$) δ 161.17, 147.81, 144.17, 137.88, 136.46, 136.07, 135.61, 131.90, 129.87, 128.18, 127.72, 127.63, 123.76, 120.51, 26.90, 21.37, 17.28. HRMS calcd for $C_{18}H_{16}N_2O$ [M+H]$^+$: 277.1341, m/z found: 277.1185.

*9, 12-dimethyl-5, 6-dihydro-8H-isoquinolino[1, 2-b]quinazolin-8-one* (**18**) Yield 1.95%, HPLC purity 98.78%, $t_R$=10.970 min。$^1$H NMR (400 MHz, DMSO-$d_6$) δ 8.40 (d, $J$=7.7 Hz, 1H), 7.56–7.34 (m, 4H), 7.14 (d, $J$=7.3 Hz, 1H), 4.23 (t, $J$=6.5 Hz, 2H), 3.10 (t, $J$=6.4 Hz, 2H), 2.76 (s, 3H), 2.57 (s, 3H). $^{13}$C NMR (101 MHz, DMSO-$d_6$) δ 161.84, 148.21, 147.31, 137.96, 137.72, 134.14, 133.35, 131.95, 129.72, 128.73, 128.11, 127.69, 127.57, 119.12, 39.27, 26.95, 23.12, 17.66. HRMS calcd for $C_{18}H_{16}N_2O$ [M+H]$^+$: 277.1341, m/z found: 277.1331.

*3-bromo-5, 6-dihydro-8H-isoquinolino[1, 2-b]quinazolin-8-one* (**23**) Yield 18.20%, HPLC purity 95.25%, $t_R$=13.216 min。$^1$H NMR (600 MHz, DMSO-$d_6$) δ 8.23 (d, $J$=71.3 Hz, 2H), 7.84 (s, 1H), 7.78–7.48 (m, 4H), 4.29 (s, 2H), 3.13 (s, 2H). $^{13}$C NMR (151 MHz, DMSO-$d_6$) δ 160.97, 149.18, 147.59, 140.57, 134.95, 130.97, 130.75, 129.86, 128.88, 127.78, 127.21, 126.81, 125.91, 120.91, 26.51. HRMS calcd for $C_{16}H_{11}BrN_2O$ [M+H]$^+$: 327.0133, m/z found: 327.0126.

*3-bromo-9-chloro-5, 6-dihydro-8H-isoquinolino[1, 2-b]quinazolin-8-one* (**25**) Yield 5.81%, HPLC purity 96.47%, $t_R$=11.081 min。$^1$H NMR (600 MHz, DMSO-$d_6$) δ 8.25 (d, $J$=8.4 Hz, 1H), 7.74 (t, $J$=7.9 Hz, 1H), 7.70–7.65 (m, 3H), 7.54 (dd, $J$=7.7, 1.2 Hz, 1H), 4.22 (t, $J$=6.5 Hz, 2H), 3.13 (t, $J$=6.5 Hz, 2H). $^{13}$C NMR (151 MHz, DMSO-$d_6$) δ 159.04, 150.07, 149.83, 140.73, 134.67, 133.10, 130.99, 130.76, 129.81, 129.48, 128.43, 127.39, 126.25, 117.84, 26.42. HRMS calcd for $C_{16}H_{10}BrClN_2O$ [M+H]$^+$: 362.9723, m/z found: 362.9710.

*3-bromo-9-bromo-5, 6-dihydro-8H-isoquinolino[1, 2-b]quinazolin-8-one* (**26**) Yield 6.10%, HPLC purity 96.54%, $t_R$=10.153 min。$^1$H NMR (600 MHz, DMSO-$d_6$) δ 8.26 (d, $J$=8.4 Hz, 1H), 7.76 (d, $J$=7.6 Hz, 1H), 7.73–7.71 (m, 2H), 7.68–7.64 (m, 2H), 4.22 (t, $J$=6.5 Hz, 2H), 3.13 (t, $J$=6.5 Hz, 2H). $^{13}$C NMR (151 MHz, DMSO-$d_6$) δ 159.17, 149.76, 140.74, 135.01, 133.26, 131.01, 130.77, 129.80, 128.50, 128.08, 126.26, 120.94, 118.89, 118.82, 26.43. HRMS calcd for $C_{16}H_{10}Br_2N_2O$ [M+H]$^+$: 406.9218, m/z found: 406.9208.

*3-bromo-9-methyl-5, 6-dihydro-8H-isoquinolino[1, 2-b] quinazolin-8-one* (**27**) Yield 10.05%, HPLC purity 98.93%, $t_R$=15.242 min。$^1$H NMR (600 MHz, DMSO-$d_6$) δ 8.25 (d, $J$=8.4 Hz, 1H), 8.22 (d, $J$=8.6 Hz, 1H), 7.69 (s, 1H), 7.66 (d, $J$=8.3 Hz, 1H), 7.33 (d, $J$=8.6 Hz, 1H), 4.24 (t, $J$=6.5 Hz, 2H), 3.12 (t, $J$=6.5 Hz, 2H), 3.00 (s, 3H). $^{13}$C NMR (151 MHz, DMSO-$d_6$) δ 160.65, 149.47, 149.10, 144.42, 142.62, 140.61, 130.98, 130.75, 129.74, 128.51, 127.79, 126.08, 120.45, 102.21, 27.91, 26.52. HRMS calcd for $C_{17}H_{13}BrN_2O$ [M+H]$^+$: 341.0290, m/z found: 341.0284.

### General procedure for the synthesis of compounds 19–22

Compounds **19–22** were synthesised as previously described[24,25]. A round-bottom flask was added with 2-aminobenzamide (**c1**–**c4**, 2 mmol), benzaldehyde (**d**, 2 mmol) and acetonitrile (8 ml). Then a catalytic amount of anhydrous $InCl_3$ (0.044 g, 0.2 mmol) was added. The reaction mixture solution was stirred at room temperature for 1–2 h and the reaction was monitored by TLC until completed. The reaction mixture was filtered and the filter cake was washed with appropriate amount of acetonitrile, then dried to give the corresponding intermediate products (**e1**–**e4**). These intermediate products were used directly without further purification.

1 mmol intermediate product were dissolved in 4 ml DMSO, then 4 mmol TBHP was added. The mixture solution was stirred at room temperature under the blue light (18 W) for 8 h and the reaction was monitored by TLC until completed. The mixture was then diluted with water (60 ml) and the precipitate was filtered off. The crude product was collected and purified by recrystallization with ethanol.

*2-phenylquinazolin-4(3H)-one* (**19**) Yield 37.50%, UPLC purity 98.14%, $t_R$=1.520 min。$^1$H NMR (600 MHz, DMSO-$d_6$) δ 12.54 (s, 1H), 8.18 (dd, $J$=15.6, 7.7 Hz, 3H), 7.84 (t, $J$=7.7 Hz, 1H), 7.75 (d, $J$=8.1 Hz, 1H), 7.61–7.52 (m, 4H).

5-chloro-2-phenylquinazolin-4(3*H*)-one (**20**) Yield 45.61%, HPLC purity 97.67%, $t_R$=7.314 min。$^1$H NMR (600 MHz, DMSO-$d_6$) δ 12.55 (s, 1H), 8.18 (s, 2H), 7.74–7.52 (m, 6H). $^{13}$C NMR (151 MHz, DMSO-$d_6$) δ 160.87, 153.46, 151.73, 134.81, 132.95, 132.59, 132.15, 129.35, 129.08, 128.30, 127.56, 118.40.

*5-bromo-2-phenylquinazolin-4(3H)-one* (**21**) Yield 98.19%, HPLC purity 99.42%, $t_R$=6.012 min。$^1$H NMR (600 MHz, DMSO-$d_6$) δ 12.56 (s, 1H), 8.18 (d, $J$=7.6 Hz, 2H), 7.73 (dd, $J$=7.8, 2.4 Hz, 2H), 7.66–7.60 (m, 2H), 7.56 (t, $J$=7.5 Hz, 2H). $^{13}$C NMR (151 MHz, DMSO-$d_6$) δ 160.97, 153.22, 151.60, 135.13, 133.10, 132.61, 132.14, 129.08, 128.29, 128.22, 120.61, 119.31.

*5-methyl-2-phenylquinazolin-4(3H)-one* (**22**) Yield 71.92%, HPLC purity 98.09%, $t_R$=9.483 min。$^1$H NMR (600 MHz, DMSO-$d_6$) δ 12.30 (s, 1H), 8.18 (d, J=7.4 Hz, 3H), 7.66 (t, J=7.7 Hz, 1H), 7.60–7.58 (m, 1H), 7.56–7.53 (m, 3H), 7.26 (d, J=7.3 Hz, 1H), 2.82 (s, 3H). $^{13}$C NMR (151 MHz, DMSO-$d_6$) δ 163.49, 152.38, 150.76, 140.44, 134.06, 132.95, 131.78, 129.36, 129.03, 128.12, 126.19, 119.78, 22.96.

### General procedure for the synthesis of compounds 24 and 28

Compounds **24** and **28** were synthesised via the Suzuki coupling reaction as previously described[26]. A mixture of $Pd(PPh_3)_4$ (43 mg, 0.034 mol), compound **23** or **25** (0.336 mmol), and $K_2CO_3$ (404 mg, 2.9 mmol) in THF/$H_2O$ (15:7) was stirred at 45 °C for 1 h under $N_2$ atmosphere. The reaction mixture was then stirred at 65 °C for 10 h after adding phenylboronic acid (**f**, 54 mg, 0.403 mmol). The reaction mixture was concentrated under reduced pressure to give the crude product, which was purified by chromatography on silica gel with dichloromethane-petroleum ether (V/V=3/1) to afford the title compounds **24** and **28**.

*3-phenyl-5, 6-dihydro-8H-isoquinolino[1, 2-b]quinazolin-8-one* (**24**) Yield 22.61%, HPLC purity 98.82%, $t_R$=9.245 min。$^1$H NMR (600 MHz, DMSO-$d_6$) δ 8.45 (d, $J$=8.2 Hz, 1H), 8.18 (d, $J$=7.9 Hz, 1H), 7.85 (t, $J$=7.6 Hz, 1H), 7.79–7.74 (m, 5H), 7.56–7.45 (m, 3H), 7.44 (t, 1H), 4.35 (t, $J$=6.5 Hz, 2H), 3.20 (t, $J$=6.5 Hz, 2H). $^{13}$C NMR (151 MHz, DMSO-$d_6$) δ 161.09, 149.66, 147.83, 143.68, 139.48, 138.84, 134.89, 129.55, 128.75, 128.57, 127.77, 127.34, 126.99, 126.80, 126.36, 125.97, 120.86, 39.76, 27.02. HRMS calcd for $C_{22}H_{16}N_2O$ [M+H]$^+$: 325.1341, m/z found: 325.1333.

*3-phenyl-9-chloro-5, 6-dihydro-8H-isoquinolino[1, 2-b]quinazolin-8-one* (**28**)Yield 47.53%, HPLC purity 96.15%, $t_R$=8.950 min。$^1$H NMR (600 MHz, DMSO-$d_6$) δ 8.42 (d, $J$=8.2 Hz, 1H), 7.79–7.74 (m, 5H), 7.70 (d, $J$=8.0 Hz, 1H), 7.52 (t, $J$=7.5 Hz, 3H), 7.44 (t, $J$=7.4 Hz, 1H),

4.28 (t, $J$=6.5 Hz, 2H), 3.20 (t, $J$=6.5 Hz, 2H). $^{13}$C NMR (151 MHz, DMSO-$d_6$) δ 159.18, 150.32, 143.97, 139.42, 139.03, 134.62, 133.08, 129.56, 129.26, 128.81, 128.55, 128.11, 127.39, 127.36, 126.36, 125.98, 117.78, 39.80, 26.92. HRMS calcd for $C_{22}H_{15}ClN_2O$ $[M+H]^+$: 359.0951, m/z found: 359.0945.

### Cell culture

Murine macrophage RAW264.7 cells, Hela cells and human hepatoma HepG2 cells were purchased from China Centre for Type Culture Collection. All cells were cultured in DMEM (Gibco) with 10% foetal bovine serum (FBS) (Gibco) and 1% 10 kU/ml penicillin/10 mg/ml streptomycin. All cells were grown in a humidified atmosphere of 5% $CO_2$ and 95% $O_2$ at 37 °C.

### ABCA1 promoter activation screening assay

The ABCA1 promoter activation screening assay was conducted as previously described in the Hela cell line, which is widely used as a model for screening active compounds that can upregulate ABCA1 expression due to its low endogenous expression level of ABCA1[27–29]. An ABCA1 promoter luciferase plasmid (pGL3-ABCA1-Luc) was constructed by cloning the human ABCA1 promoter region (–819 bp to +71 bp) into the pGL3-basic vector (Promega Corporation) according to the previous report[30]. Hela cells were grown overnight and then transiently co-transfected with the plasmids of pGL3-ABCA1-Luc and pRL-SV40 (Promega Corporation) using a transfection reagent Lipofectamine 2000 (Thermo Fisher Scientific Inc) following the manufacturer's guidelines. 6 h later, the transfection solution was removed and the cells were treated with the tested compounds for 24 h. The LXR agonist T0901317 and rutaecarpine served as positive controls, while 0.1% DMSO was utilised as the vehicle control. Then the cells were lysed, and the activities of firefly and renilla luciferase were measured subsequently using the dual luciferase reporter gene assay kit (Beyotime Biotechnology). The results were presented as relative firefly luciferase activity, normalised to the Renilla luciferase signal (calculated as fold change compared to the vehicle control).

### RNA extraction and real-time PCR assay

RAW264.7 Cells were lysed with TRIZOL reagent and total RNA was extracted to determine RNA concentration. cDNA was prepared from RNA samples using a reverse transcription kit according to the manufacturer's protocol. Real-Time quantitative PCR was performed with the above prepared cDNA and SYBR Green Master Mix on the ABI Prism 7500 Sequence Detection System (Applied Biosystems, Foster City, CA, USA), SYBR Green I Real-Time PCR kit (Roche Diagnostics). Relative changes in gene expression were calculated by using the comparative threshold cycle (ΔΔCt) method, and β-actin was used as the internal control gene. The primer sequences of each gene used for the experiment are shown as follows:

ABCA1 forward primer, 5′-GGGTCTGAACTGCCCTACCT-3′

ABCA1 reverse primer, 5′-TACTCCCCTGATGCCACTTC-3′

β-actin forward primer, 5′-CTAAGGCCAACCGTGAAAG-3′

β-actin reverse primer, 5′-ACCAGAGGCATACAGGGACA-3′

### Western blotting assay

RAW264.7 Cells were lysed with RIPA lysis solution to collect total proteins. The cell lysate was centrifuged at 12000 rpm for 15 min at 4 °C and protein concentrations of the supernatants were determined using the BCA protein concentration assay kit (Beyotime Biotechnology). 5x loading buffer was added and boiled to denature the proteins. All protein samples were separated by SDS-PAGE and transferred onto PVDF membranes by wet transfer. The samples were then incubated with the corresponding primary antibody (1:1000) overnight at 4 °C, washed three times with TBST and then incubated with the corresponding secondary antibody (1:5000) for 2 h at room temperature on a shaker. After three washes with TBST, the exposure time was adjusted on the chemiluminescence imaging system. The immunoreactive protein bands were then visualised and examined.

### Ox-LDL induced lipid accumulation and foam cell formation assay

The lipid uptake and foam cell formation assay was performed as previously described[21,28,31]. RAW264.7 cells were grown in a 96-well plate and cultured with serum-free DMEM for 24 h at 37 °C. Then the cells were incubated with serum-free DMEM containing ox-LDL or DiI-ox-LDL (80 μg/mL) for another 24 h. The tested compounds were then added to the cells. Rutaecarpine (10 μM) was used as the positive control, 0.1% DMSO was used as the vehicle control. After 24 h, the cells were fixed in 4% formaldehyde for 20 min, rinsed with PBS, and immersed in 60% 2-propanol. Then the cells were stained with oil red O in 60% 2-propanol (0.3%, w/v) for 15 min. After three additional washes with PBS, the cell nuclei were subsequently stained with haematoxylin for 2 min and then washed three times with PBS. The prepared samples were added with PBS and examined under a light microscope.

For the fluorescence analysis, cell nucleui were stained with DAPI and intracellular fluorescent labelled-lipids were then examined under a fluorescence microscope.

### Hepatic lipid accumulation assay

The hepatic lipid accumulation assay was performed as previously described with slight modification[28]. For lipid staining, HepG2 cells were cultured in a 24-well plate overnight at 37 °C, followed by treatment with the compounds for 48 h. The cells were then fixed in 4% formaldehyde for 20 min, rinsed with PBS, and immersed in 60% 2-propanol. Next, the cells were stained with oil red O in 60% 2-propanol (0.3%, w/v) for 15 min. After three additional washes with PBS, the prepared samples were added with PBS and examined under a light microscope. For measuring intracellular triglyceride levels, HepG2 cells were grown in a 6-well plate overnight at 37 °C and treated with the compounds for 48 h. The cells were lysed, and triglyceride concentrations were assessed using a triglyceride assay kit according to the manufacturer's instructions.

### MTT assay

The 3–(4, 5-dimethylthiazol-2-yl)-2,5-diphenyltetrazolium (MTT) assay was performed as previously described[32]. RAW264.7 cells, Hela cells and human hepatoma HepG2 cells were plated at 5000 cells per well and allowed to grow at 37 °C overnight. Then the cells were treated with various concentrations of the tested

compound for 24 h, 0.1% DMSO was used as the vehicle control. After the treatment, the cell culture medium was then removed, followed by the addition of fresh cell culture medium containing 5.0 g/L MTT (20 µL/per well) and incubation at 37 °C in a humidified, 5% $CO_2$ atmosphere for 4 h. After removal of the supernatant, 150 µL of DMSO was added to each well to dissolve the formed formazan crystals. Then the absorbance was measured at 570 nm in a multi-well plate reader. The results are expressed as % relative cell viability compared to vehicle control.

## Results

### *Chemistry*

The polycyclic fused quinazolinone compounds **1**–**18**, **23**, **25**–**27** were synthesised as illustrated in Scheme 1. Various substituted isatins were used to react with 1, 2, 3, 4-tetrahydroisoquinoline in the presence of TBHP. It is proposed that the isatins were initially oxidised to isatoic anhydrides, while the 1, 2, 3, 4-tetrahydroisoquinoline was also oxidised to dihydroisoquinoline. Both intermediates subsequently underwent decarboxylative cyclisation, and the resulting intermediate products were then sequentially oxidised to yield the final products[23,33]. Most of these compounds were obtained with low yields, which might be likely due to the formation of excess byproducts.Compounds **19**–**22** was synthesised as illustrated in Scheme 2. First, intermediate products **B1**–**B4** were prepared by reacting various substituted 2-aminobenzamides **A1**–**A4** with benzaldehydes. The reaction of cyclisation was catalysed by $InCl_3$. Then these intermediates were further oxidised by TBHP under the blue light (18W) to give the desired compounds with yields of 37.5% to 98.2%.

Compounds **24** and **28** were synthesised as illustrated in Scheme 3. The -Br group of compounds **23** and **25** was substituted with the phenyl moiety via the Suzuki coupling reaction, catalysed by $Pd[(Ph)_3P]_4$ and $K_2CO_3$ in the presence of phenylboronic acid. The desired compounds were obtained with yields of 22.61% and 47.53%, respectively.

### *The screening assay of ABCA1 promoter activation*

All the synthetic compounds were firstly screened for the activation activity on the ABCA1 promoter using a reporter gene assay. The LXR agonist T0901317 and rutaecarpine were used as positive controls, 0.1% DMSO as the vehicle control. The tested concentration of compounds was 10 µM unless otherwise stated. The activity is expressed as relative luciferase activity, normalised to the Renilla

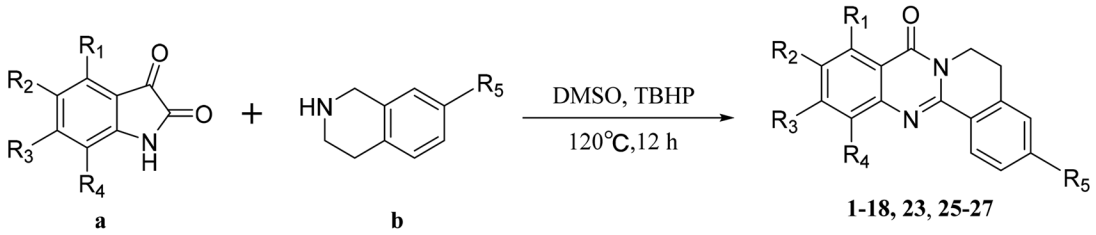


| Entry | $R_1$ | $R_2$ | $R_3$ | $R_4$ | $R_5$ | Entry | $R_1$ | $R_2$ | $R_3$ | $R_4$ | $R_5$ |
|---|---|---|---|---|---|---|---|---|---|---|---|
| **1** | H | H | H | H | H | **12** | H | H | $OCH_3$ | H | H |
| **2** | Cl | H | H | H | H | **13** | H | H | H | Cl | H |
| **3** | Br | H | H | H | H | **14** | H | H | H | F | H |
| **4** | $CH_3$ | H | H | H | H | **15** | H | H | H | $CH_3$ | H |
| **5** | H | F | H | H | H | **16** | H | H | H | $CF_3$ | H |
| **6** | H | Cl | H | H | H | **17** | H | $CH_3$ | H | $CH_3$ | H |
| **7** | H | Br | H | H | H | **18** | $CH_3$ | H | H | $CH_3$ | H |
| **8** | H | $CH_3$ | H | H | H | **23** | H | H | H | H | Br |
| **9** | H | $OCH_3$ | H | H | H | **25** | Cl | H | H | H | Br |
| **10** | H | H | Cl | H | H | **26** | Br | H | H | H | Br |
| **11** | H | H | Br | H | H | **27** | $CH_3$ | H | H | H | Br |

Scheme 1. Synthesis of compounds **1–18**, **23**, **25–27**.

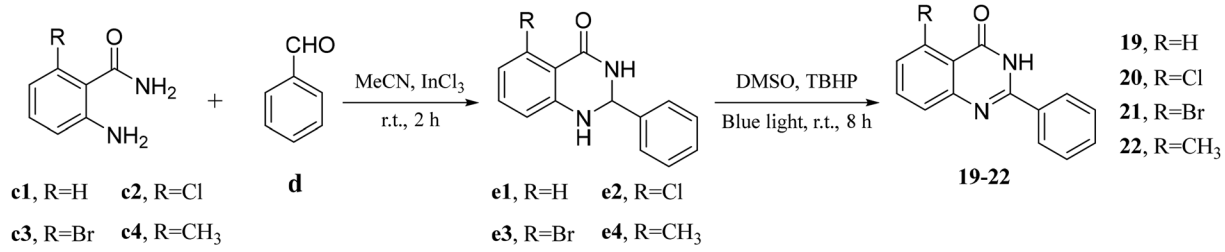


Scheme 2. Synthesis of compounds **19–22**.

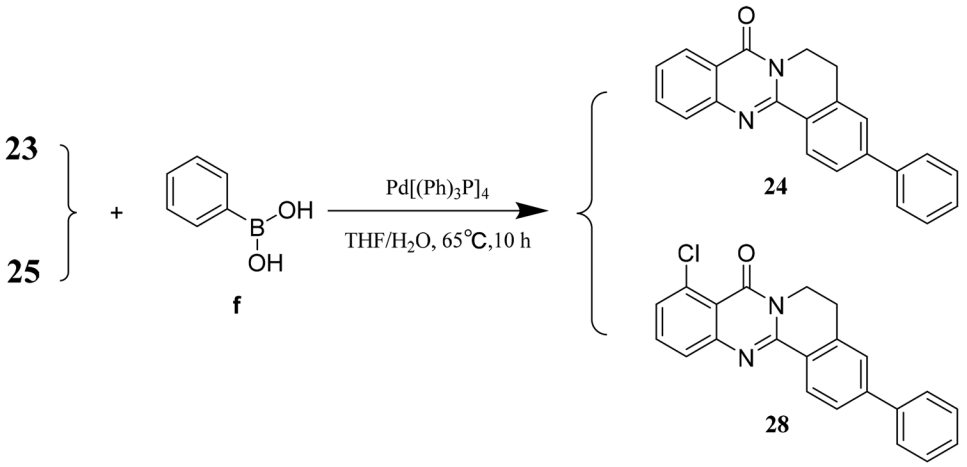


**Scheme 3.** Synthesis of compounds **24** and **28**.

**Table 1.** ABCA1 promoter activation induced by compounds **1**–**28**.

| Compound | ABCA1 promoter activation (±SD)[a] | Compound | ABCA1 promoter activation (±SD)[a] |
|---|---|---|---|
| T0901317 | 3.20 ± 0.30[b] | **14** | 0.94 ± 0.07 |
| rutaecarpine | 2.57 ± 0.30 | **15** | 0.99 ± 0.14 |
| **1** | 1.10 ± 0.09 | **16** | 0.87 ± 0.07 |
| **2** | 2.00 ± 0.25 | **17** | 1.15 ± 0.08 |
| **3** | 2.50 ± 0.13 | **18** | 1.07 ± 0.03 |
| **4** | 1.75 ± 0.19 | **19** | 1.13 ± 0.07 |
| **5** | 1.14 ± 0.10 | **20** | 1.36 ± 0.10 |
| **6** | 0.99 ± 0.10 | **21** | 1.26 ± 0.11 |
| **7** | 1.04 ± 0.00 | **22** | 1.35 ± 0.06 |
| **8** | 1.09 ± 0.13 | **23** | 1.13 ± 0.16 |
| **9** | 1.14 ± 0.09 | **24** | 0.67 ± 0.05 |
| **10** | 0.88 ± 0.05 | **25** | 1.43 ± 0.11 |
| **11** | 1.23 ± 0.10 | **26** | 1.59 ± 0.28 |
| **12** | 1.01 ± 0.12 | **27** | 0.91 ± 0.18 |
| **13** | 1.38 ± 0.12 | **28** | 0.63 ± 0.08 |

[a]Fold activation of the tested compounds (10 μM) compared to vehicle control, where the mean relative firefly luciferase activity is normalised to the Renilla luciferase signal. Data are represented as means ± (SD) of at least three independent experiments performed in triplicate.
[b]ABCA1 promoter activation at 0.1 μM.

luciferase signal. ABCA1 promoter activation for the vehicle control was defined as 1-fold activation.

The screening results were summarised in Table 1. As expected, the positive controls T0901317 induced a significant activation with the response of 3.2-fold over the vehicle control at 0.1 μM. Rutaecarpine also induced a 2.57-fold activation response over the vehicle control at 10 μM, which was consistent with the previous report[21]. For the 5, 6-dihydro-8*H*-isoquinolino[1, 2-*b*]quinazolin-8-one derivatives, the parent compound **1** exhibited little activation activity (1.10-fold). The effects of structural modifications on the parent compound's activities were given as follows:

For the phenyl ring of the quinazolinone moiety of compound **1**, when introducing the halogen atoms -Cl, -Br or the -$CH_3$ group to the C-9 position, the resulted compounds **2**, **3**, **4** exhibited significant increased activation activity. Compound **2** and **4** showed 2.00- and 1.75-fold activation. Compound **3** demonstrated the most potent activation activity in this series of compounds, with the activation response of 2.50-fold over the vehicle control, which was comparable to that of rutaecarpine. Introduction of various substituents such as -F, -Cl, -Br, -$CH_3$, -$OCH_3$ to the C-10 position at the A ring of compound **1** (compound **5**, **6**, **7**, **8**, **9**) did not increase the activation activity. Similarly, introduction of -Cl, -Br and -$OCH_3$ to the C-11 position (compound **10**, **11**, **12**) did not induce apparent activation activity as well. Although introduction of -Cl to the C-12 position induced a slight increase activation activity (compound **13**, 1.38-fold), introducing -F, -$CH_3$ and -$CF_3$ at the same position (compound **14–17**) did not induce any activation activity. Considering that introduction of -$CH_3$ to the C-12 position at the A ring of compound **4** dramatically decreased the activation activity (compound **18**, 1.07-fold), we concluded that introduction of halogen atoms or the methyl group at the C-9 position, rather than other positions of the A ring, were favourable to increase the activation activity and the bromine atom would be preferable.

For the piperidine ring of tetrahydroisoquinoline moiety of compound **1**, cleaving this conjugated ring did not increase the activation activity (compound **19**, 1.13-fold). Furthermore, cleaving the piperidine ring of the active compounds **20**, **21**, **22** dramatically decreased the activation activity when compared to that of corresponding compounds. These results suggested that the piperidine ring of 5, 6-dihydro-8*H*-isoquinolino[1, 2-*b*]quinazolin-8-one derivatives was necessary for the activation activity.

For the phenyl ring of tetrahydroisoquinoline moiety of compound **1**, introduction -Br or the phenyl group to the C-3 position led to compound **23**–**24**, which show little or no activation activity. Introduction -Br or the phenyl group at the same position to the active compounds **2**, **3** and **4**, the resulted compounds **25**, **26**, **27** and **28** exhibited marked decreased activation activity compared to the corresponding compounds. These results suggested that introducing substituents to the C-3 position are not tolerant.

Taking together, an overview of the SAR of the 5, 6-dihydro-8*H*-isoquinolino[1, 2-*b*]quinazolin-8-one derivatives with respect to ABCA1 promoter activation was provided in Figure 2.

To further evaluate the effect of the hit on ABCA1 promoter activation, the most potent compound **3** was selected and various concentrations of this compound were applied to the RAW264.7 cells. As illustrated in Figure 3(A), compound **3** could activate the ABCA1 promoter in a dose-dependent manner.

### *Compound 3 up-regulated ABCA1 mRNA and protein levels in RAW264.7 macrophage cells*

To investigate the upregulation of ABCA1 by compound **3**, RAW 264.7 macrophages were incubated with various concentrations of compound **3** and the intracellular levels of ABCA1 mRNA and protein were determined.

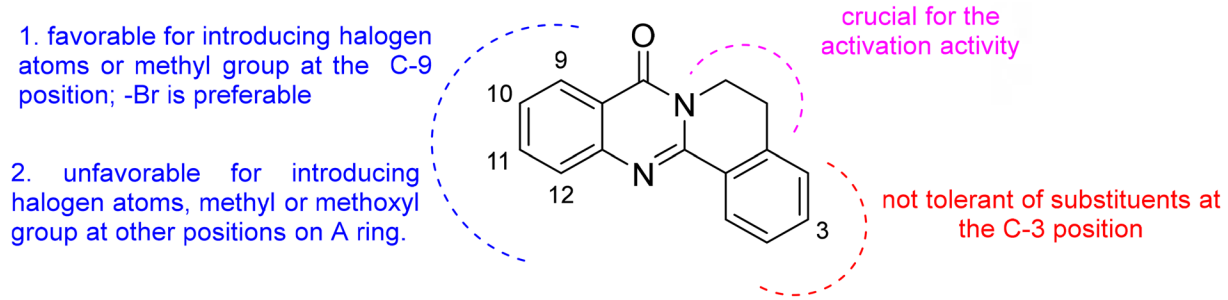


**Figure 2.** The SAR of 5, 6-dihydro-8*H*-isoquinolino[1, 2-*b*]quinazolin-8-one compounds on ABCA1 promoter activation.

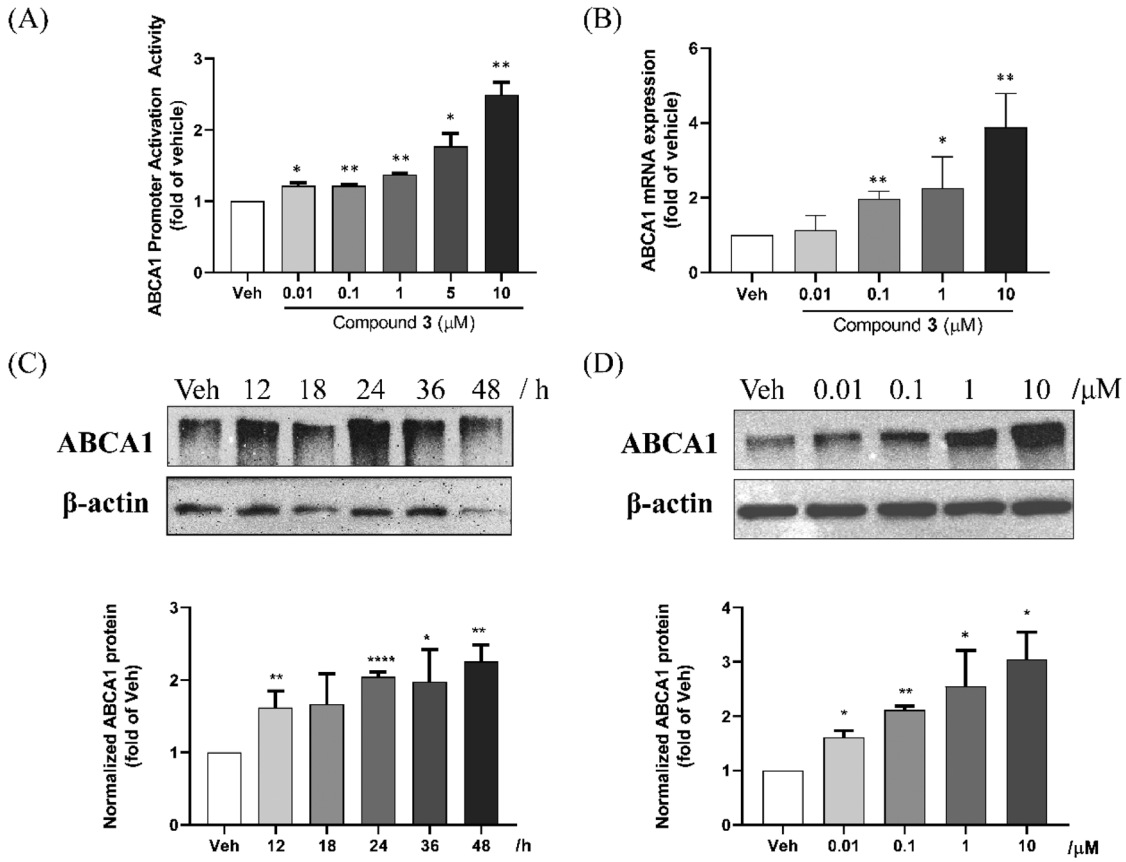


**Figure 3.** Effects of compound **3** on the expression of ABCA1 in Hela and RAW264.7 cells. (A), Dose-dependent effects on the activation of ABCA1 promoter upon treatment with **3** in Hela cells; (B), Dose-dependent effects of compound **3** on the mRNA expression of ABCA1 in RAW264.7 cells; (C), Time-dependent effects of compound **3** on the protein expression of ABCA1 in RAW264.7 cells after treatment with compound **3** at 10 μM for the indicated time; (D) Dose-dependent effects of compound **3** on the protein expression of ABCA1 in RAW264.7 cells after treatment with compound **3** at various concentrations for 24 h. Bands from time-dependent blots and dose-response blots were quantified by densitometry, normalised to β-actin, and expressed as fold of vehicle treatment. Data are represented as mean ± SD from at least two independent experiments. Veh, 0.1% DMSO. Significance: *$p < 0.05$, **$p < 0.01$, ****< 0.0001, vs. vehicle group.

For the analysis of ABCA1 gene expression, real-time PCR was performed. RAW 264.7 cells were incubated with various concentrations of compound **3** (0.01–10 μM) for 18 h, then the mRNA expression of ABCA1 was examined. The data shown in Figure 3(B) indicated that compound **3** could effectively induce the mRNA expression of ABCA1 in a dose-dependent manner with a maximum increase of 3.94-fold of control at 10 μM.

For the analysis of ABCA1 protein expression, the time-dependent expression assay was performed first to determine the time of maximal expression. RAW264.7 cells were treated with compound **3** at the concentration of 10 μM for 12, 18, 24, 36 and 48 h, then the expression of ABCA1 protein was analysed. As shown in Figure 3(C), ABCA1 protein in RAW264.7 cells were increased by compound **3** at the concentration of 10 μM with the maximum responses from 24 h to 48 h (2.0–2.2 fold increase compared to the vehicle group). RAW264.7 cells were therefore treated with various concentrations (0.01–10 μM) of compound **3** for 24 h. As expected, ABCA1 expression was significantly up-regulated upon treatment with compound **3** (1.6–3.0 fold increase compared to the vehicle group), exhibiting a dose-dependent response at concentrations ranging from 0.01 to 10 μM (Figure 3(D)).

The above results confirmed that the ABCA1 promoter activator **3** could effectively increase the expressions of ABCA1 mRNA and protein in RAW264.7 cells.

### *Compound 3 upregulated the expression of ABCA1 by targeting the LXR-involved pathway*

It is well known that the expression of ABCA1 is transcriptionally regulated by various nuclear receptors, particularly LXR. To investigate the potential mechanism of the active compound, the typical LXR antagonist GSK2033 was utilised to examine its effect on the up-regulation of ABCA1 induced by compound **3**. As illustrated in Figure 4, GSK2033 could completely abolished the activation on ABCA1 promoter and the up-regulation of ABCA1 protein induced by compound **3**. These results indicated that compound **3** upregulated the expression of ABCA1 by targeting the LXR-involved pathway.

### *Compound 3 reduced ox-LDL-induced lipid accumulation and inhibited foam cell formation*

To evaluate the effects of compound **3** on reducing lipid accumulation in macrophage cells and inhibiting foam cell formation, a foam cell model was established in this experiment by incubating RAW264.7 cells with 80 μg/ml ox-LDL or Dil-ox-LDL for 24 h. The lipid droplets in cells could be stained with oil red O and examined under a light microscopy. The fluorescent label-lipid droplets could be visualised under a fluorescence microscope.

As illustrated in Figures 5 and 6, compared to the control groups (Figures 5(A) and 6(A)), treating the RAW 264.7 cells with ox-LDL or Dil-ox-LDL induced the formation of foam cells, characterised by an abundance of lipid droplets surrounding the nuclei (Figures 5(B) and 6(B))[21]. When treating the foam cells with the positive control rutaecarpine (10 μM), the intracellular lipid droplets were noticeably reduced compared to the model groups (Figures 5(C) and 6(C)), which was consistent with the previous report[21]. As for the compound **3**, treatment of the foam cells with **3** (10 μM) for 24 h also resulted in a significant reduction of the lipid droplets in the cell plasma (Figures 5(D) and 6(D)). The above results clearly suggested that compound **3** could effectively reduce ox-LDL-induced intracellular lipid accumulation and inhibit foam cell formation.

### *Compound 3 induced limited lipid and triglyceride accumulation in HepG2 cells*

To investigate the effects of compound **3** on triglyceride synthesis and lipogenesis in hepatic cells, HepG2 cells were incubated with the tested compounds for 48 h. Intracellular lipid accumulation was stained using oil red O and examined under a light microscopy. The staining results revealed that the positive control T0901317 caused a significant increased accumulation of lipid droplets in the cytoplasm of HepG2 cells compared to the vehicle control (Figure 7(A) and (B)). In contrast, being similar to the effect of rutaecarpine (Figure 7(C)), treatment with compound **3** resulted in minimal lipid droplets formation in these cells (Figure 7(D)).

Additionally, intracellular triglyceride levels of HepG2 cells were also measured. As shown in Figure 8(A), after 48 h, T0901317 increased triglyceride levels by 49% over the vehicle control at the concentration of 0.1 μM. Conversely, compound **3** did not increase the triglyceride level in HepG2 cells even at the concentration of 10 μM.

The above findings suggested that compound **3** induced limited lipid and triglyceride accumulation in HepG2 cells, potentially avoiding the side effects associated with hypertriglyceridaemia and hepatic lipogenesis.

### *Cell cytotoxicity assay*

The cytotoxicity of compound **3** was assessed in Hela, RAW264.7, and HepG2 cells using the MTT assay. As shown in Figure 8(B), across all tested cell lines, there was no significant decrease in cellular viability induced by compound **3** even at the highest tested concentration (10 μM). These results indicated that the active compound **3** exhibited low cytotoxicity, and errors resulting from cytotoxic effects were eliminated in the present studies.

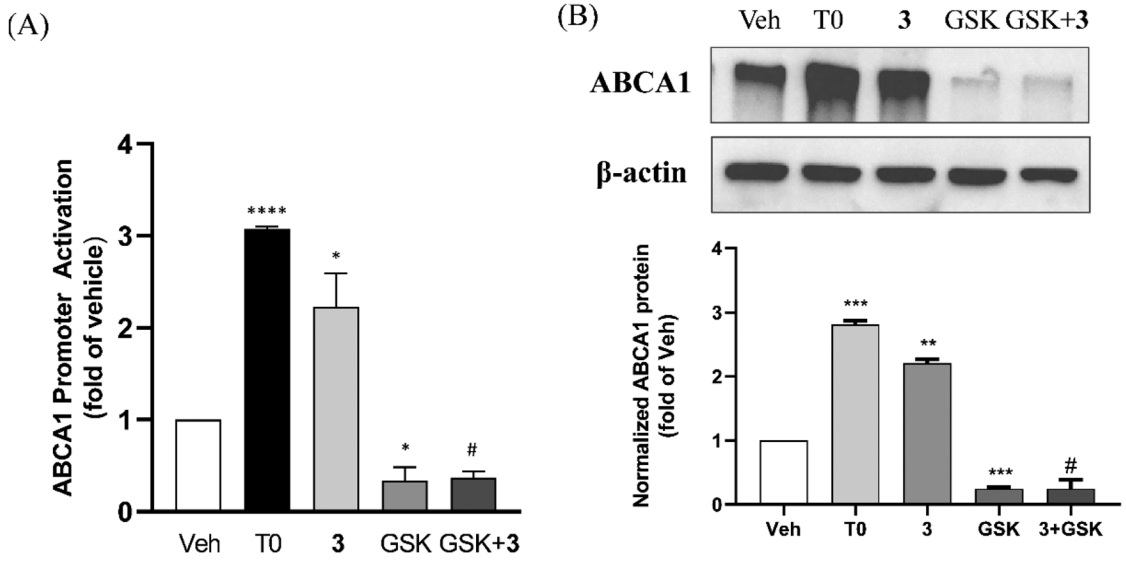


**Figure 4.** Suppressing effects of GSK2033 on the up-regulation of ABCA1 induced by compound **3**. (A) Suppressing effects on the activation of ABCA1 promoter upon treatment with T0901317 (0.1 μM), **3** (10 μM), GSK2033 (1 μM) and **3** together with GSK2033 in Hela cells; (B) Suppressing effects on the expression of ABCA1 protein upon treatment with T0901317 (0.1 μM), **3** (10 μM), GSK2033 (1 μM) and **3** together with GSK2033 in RAW264.7 cells. Bands from western blots were quantified by densitometry, normalised to β-actin, and expressed as fold of vehicle treatment. Data are represented as mean ± SD from at least two independent experiments. Veh, 0.1% DMSO; T0, T0901317; GSK, GSK2033. Significance: *$p < 0.05$, **$p < 0.01$, ***$p < 0.001$, ****$p < 0.0001$, vs. vehicle group; #$p < 0.01$, vs. compound **3** treated-group.

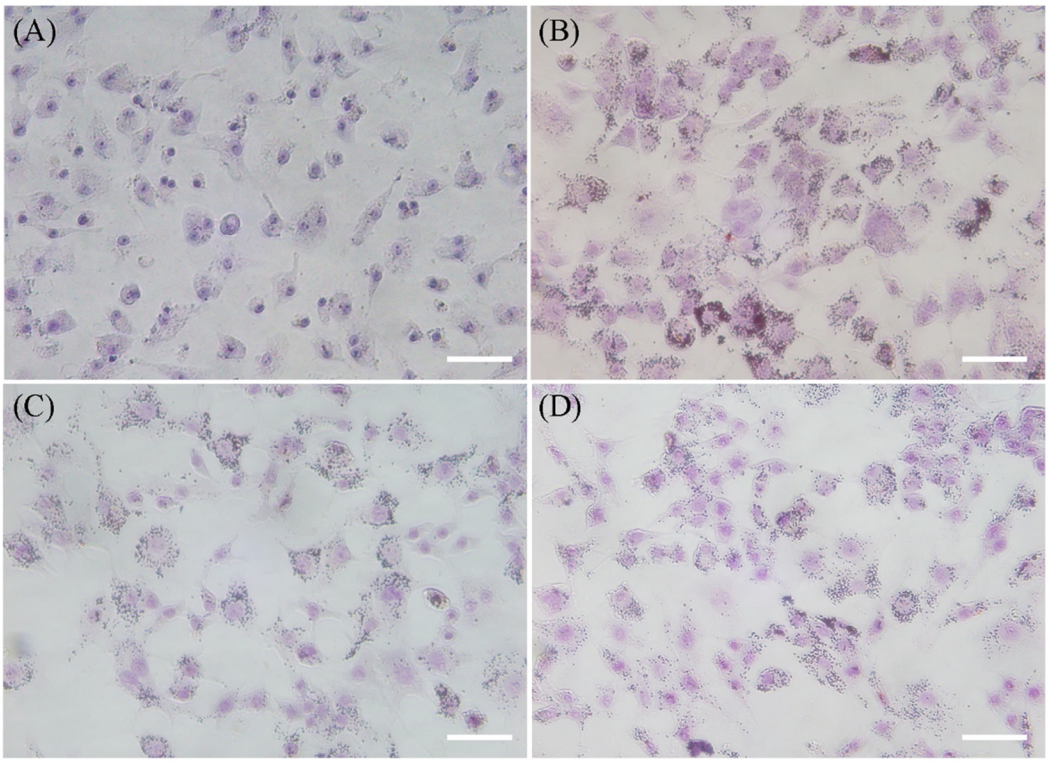


**Figure 5.** Inhibitory effects of compound **3** on the lipid accumulation in the ox-LDL stimulated RAW264.7 macrophages. RAW264.7 macrophages were incubated with serum-free DMEM (A) or serum-free DMEM containing 80 μg/mL ox-LDL for 24 h (B-D). Then the cells were treated with 0.1% DMSO (B), rutaecarpine (10 μM, C) and compound **3** (10 μM, D) for 24 h. Intracellular lipid droplets were stained with oil red O, and cell nucleui were stained with haematoxylin staining solution. Images of the stained cells were captured using 40× objective. Scale bar: 50 μm.

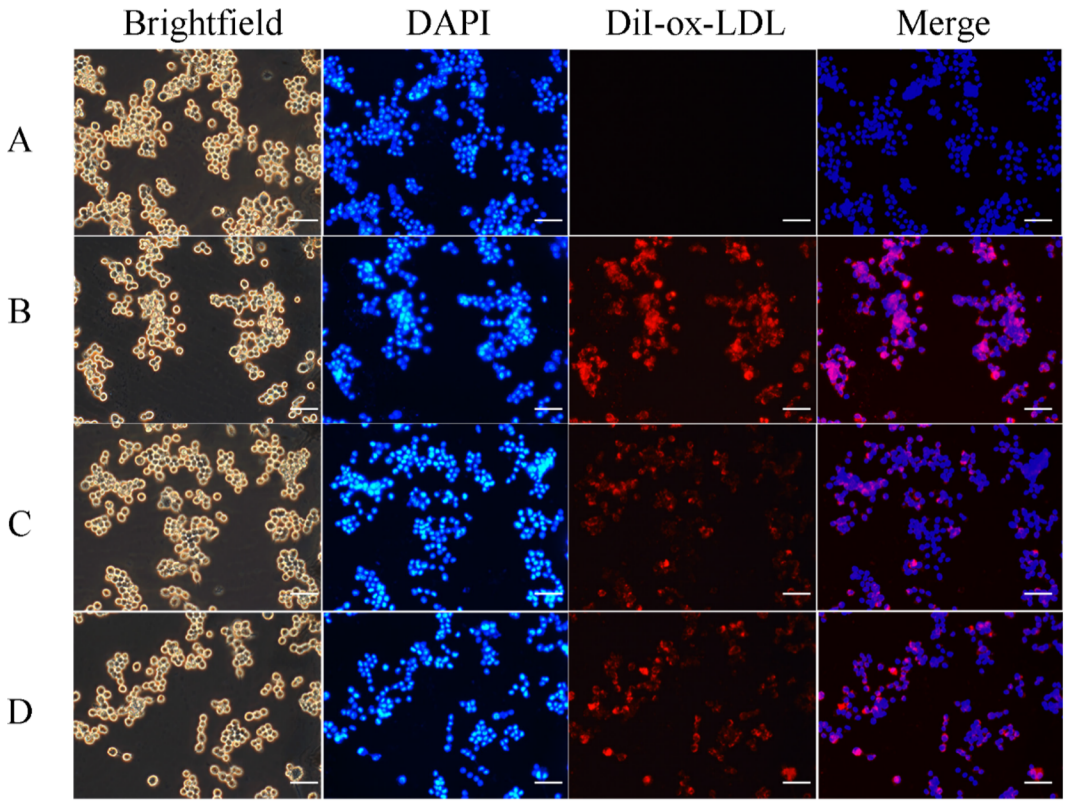


**Figure 6.** Inhibitory effects of compound **3** on the lipid accumulation in the DiI-ox-LDL stimulated RAW264.7 macrophages. RAW264.7 macrophages were incubated with serum-free DMEM (A) or serum-free DMEM containing 80 μg/mL DiI-ox-LDL for 24 h (B-D). Then the cells were treated with 0.1% DMSO (B), rutaecarpine (10 μM, C) and compound **3** (10 μM, D) for 24 h. Cell nucleui were stained with DAPI. Intracellular fluorescent labelled-lipids were then examined under a fluorescence microscope. Images of the stained cells were captured using 40× objective. Scale bar: 50 μm.

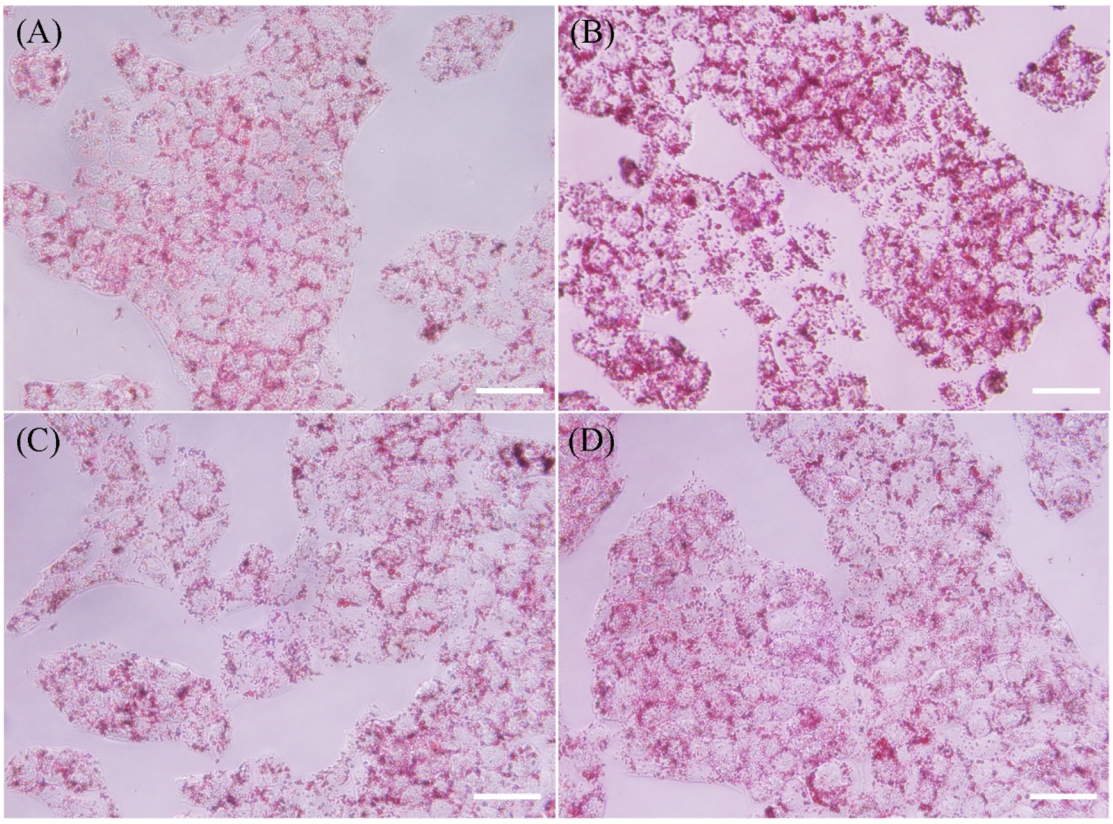


**Figure 7.** Effects of compound **3** on the lipid accumulation in HepG2 cells. HepG2 cells were treated with rutaecarpine and compound **3** at 10 μM for 48 h, 0.1 μM T0901317 was used as the positive control, 0.1% DMSO was used as the vehicle control. Intracellular lipid droplets were then stained with oil red O. Images of the stained cells were captured using 40× objective. Scale bar: 50 μm. (A), the vehicle group; (B), the T0901317-treated group; (C), the rutaecarpine-treated group; (D), the compound **3**-treated group.

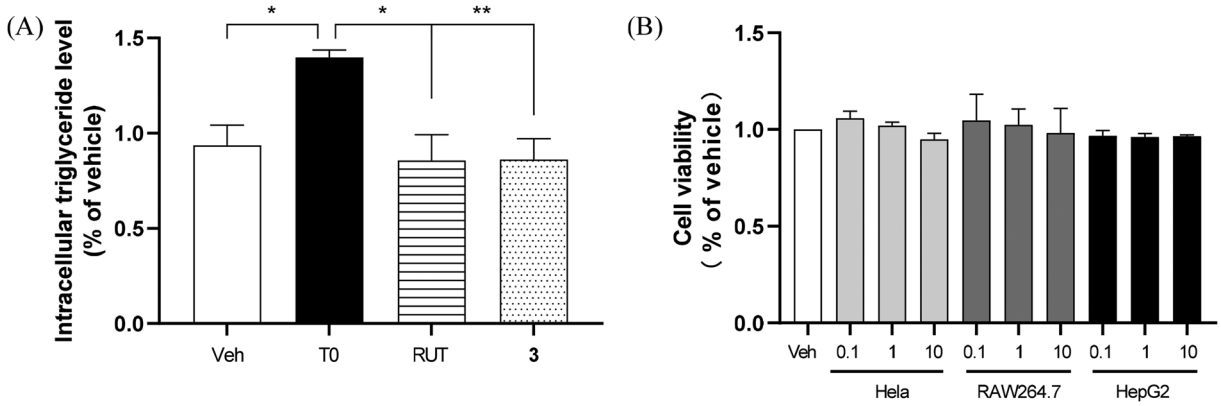


**Figure 8.** (A) Effects of T0901317 (0.1 μM), rutaecarpine and compound **3** (10 μM) on the triglyceride synthesis in HepG2 cells. The data represented are average values of at least two independent experiments (mean ± SD). Veh, vehicle; T0, T0901317; RUT, rutaecarpine. (B) Cell viability of Hela, RAW264.7 and HepG2 cells after treatment with compound **3** at the concentrations of 0.1–10 μM for 24 h. Significance: $^{*}p < 0.05$, $^{**}p < 0.01$.

## Conclusion

In this study, a series of 5, 6-dihydro-8*H*-isoquinolino[1, 2-*b*] quinazolin-8-one derivatives were synthesised and evaluated as potential activators of ABCA1 promoter using a reporter gene assay. SAR analysis indicated that introduction of halogen atoms at the C-9 position of the core structure significantly enhanced activation activity, with the bromine atom being the preferred substituent. Compound **3** was the most potent compound identified in this work. This compound could effectively increase ABCA1 expression in RAW264.7 cells and reduce intracellular lipid accumulation induced by ox-LDL, thereby inhibiting foam cell formation. The mechanism study revealed that compound **3** upregulated the expression of ABCA1 by targeting the LXR-involved pathway. However, compared to the LXR dual agonist T0901317, compound **3** resulted in minimal undesired lipid and triglyceride accumulation in HepG2 cells. Therefore, our findings provide a promising avenue for discovering novel ABCA1 up-regulators that can inhibit macrophage-derived foam cell formation while minimising the side effects of hypertriglyceridaemia and hepatic lipogenesis.

## Authors' contributions

Changhuan Yang performed compound synthesis and biological assays. Lin Chen contributed to biological assays. Yanmei Jiang and Demeng Sun contributed to compound synthesis. Yun Hu supervised the study, drafted and finalised the manuscript. All authors have given approval to the final version of the manuscript and agree to be accountable for all aspects of the work.

## Disclosure statement

No potential conflicts of interest were reported by the author(s).

## Funding

This work was supported by the National Natural Science Foundation of China under Grant [No. 81560562 and 21762055] and the Science and Technology Department of Guizhou Province under grant (QKHJC-ZK[2024]YB288).

## Data availability statement

The data that support the findings of this study are available from the corresponding author upon reasonable request.

## References

1. Wang D, Yang Y, Lei Y, Tzvetkov NT, Liu X, Yeung AWK, Xu S, Atanasov AG. Targeting foam cell formation in atherosclerosis: therapeutic potential of natural products. Pharmacol Rev. 2019;71(4):596–670.
2. Unit CTSUaES. Efficacy and safety of cholesterol-lowering treatment: prospective meta-analysis of data from 90 056 participants in 14 randomised trials of statins. Lancet. 2005; 366(9493):1267–1278.
3. Law MR, Wald NJ, Rudnicka AR. Quantifying effect of statins on low density lipoprotein cholesterol, ischaemic heart disease, and stroke: systematic review and meta-analysis. BMJ. 2003;326(7404):1423.
4. Kawai K, Kawakami R, Finn AV, Virmani R. Differences in stable and unstable atherosclerotic plaque. Arterioscler Thromb Vasc Biol. 2024;44(7):1474–1484.
5. Moore KJ, Tabas I. Macrophages in the pathogenesis of atherosclerosis. Cell. 2011;145(3):341–355.
6. Maguire EM, Pearce SWA, Xiao Q. Foam cell formation: a new target for fighting atherosclerosis and cardiovascular disease. Vascul Pharmacol. 2019;112(:54–71.
7. Moore KJ, Sheedy FJ, Fisher EA. Macrophages in atherosclerosis: a dynamic balance. Nat Rev Immunol. 2013;13(10):709–721.
8. Maxfield FR, Tabas I. Role of cholesterol and lipid organization in disease. Nature. 2005;438(7068):612–621.
9. Tabas I, García-Cardeña G, Owens GK. Recent insights into the cellular biology of atherosclerosis. J Cell Biol. 2015;209(1):13–22.
10. Sun Y, Li X. Cholesterol efflux mechanism revealed by structural analysis of human ABCA1 conformational states. Nat Cardiovasc Res. 2022;1(3):238–245.
11. Phillips MC. Molecular mechanisms of cellular cholesterol efflux. J Biol Chem. 2014;289(35):24020–24029.
12. Ouimet M, Barrett TJ, Fisher EA. HDL and reverse cholesterol transport: basic mechanisms and their roles in vascular health and disease. Circ Res. 2019;124(10):1505–1518.
13. El Khoury P, Couvert P, Elbitar S, Ghaleb Y, Abou-Khalil Y, Azar Y, Ayoub C, Superville A, Guérin M, Rabès J-P, et al. Identification of the first Tangier disease patient in Lebanon carrying a new pathogenic variant in ABCA1. J Clin Lipidol. 2018;12(6):1374–1382.
14. Costet P, Luo Y, Wang N, Tall AR. Sterol-dependent transactivation of the ABC1 promoter by the liver X receptor/retinoid X receptor. J Biol Chem. 2000;275(36):28240–28245.
15. Matsuo M. ABCA1 and ABCG1 as potential therapeutic targets for the prevention of atherosclerosis. J Pharmacol Sci. 2022; 148(2):197–203.
16. Tice CM, Noto PB, Fan KY, Zhuang L, Lala DS, Singh SB. The medicinal chemistry of liver X receptor (LXR) modulators. J Med Chem. 2014;57(17):7182–7205.
17. El-Gendy BE-DM, Goher SS, Hegazy LS, Arief MMH, Burris TP. Recent advances in the medicinal chemistry of liver X receptors. J Med Chem. 2018;61(24):10935–10956.
18. Lund EG, Menke JG, Sparrow CP. Liver X receptor agonists as potential therapeutic agents for dyslipidemia and atherosclerosis. Arterioscler Thromb Vasc Biol. 2003;23(7):1169–1177.
19. Hong C, Tontonoz P. Liver X receptors in lipid metabolism: opportunities for drug discovery. Nat Rev Drug Discov. 2014; 13(6):433–444.
20. Ben Aissa M, Lewandowski CT, Ratia KM, Lee SH, Layden BT, LaDu MJ, Thatcher GRJ. Discovery of nonlipogenic ABCA1 inducing compounds with potential in Alzheimer's disease and type 2 diabetes. ACS Pharmacol Transl Sci. 2021;4(1):143–154.
21. Xu Y, Liu Q, Xu Y, Liu C, Wang X, He X, Zhu N, Liu J, Wu Y, Li Y, et al. Rutaecarpine suppresses atherosclerosis in Apoe−/− mice through upregulating ABCA1 and SR-BI within RCT. J Lipid Res. 2014;55(8):1634–1647.
22. Albers M, Blume B, Schlueter T, Wright MB, Kober I, Kremoser C, Deuschle U, Koegl M. A novel principle for partial agonism of liver X receptor ligands: competitive recruitment of activators and repressors. J Biol Chem. 2006;281(8):4920–4930.
23. Chen X, Xia F, Zhao Y, Ma J, Ma Y, Zhang D, Yang L, Sun P. TBHP-mediated oxidative decarboxylative cyclization in water: direct and sustainable access to anti-malarial polycyclic fused quinazolinones and rutaecarpine. Chin J Chem. 2020; 38(11):1239–1244.
24. Mulakayala N, Kandagatla B, Ismail, Rapolu RK, Rao P, Mulakayala C, Kumar CS, Iqbal J, Oruganti S. $InCl_3$-catalysed synthesis of 2-aryl quinazolin-4(3*H*)-ones and 5-aryl pyrazolo[4,3-d]pyrimidin-7(6*H*)-ones and their evaluation as potential anticancer agents. Bioorg Med Chem Lett 2012; 22(15): 5063–5066.
25. Xie Z, Lan J, Zhu H, Lei G, Jiang G, Le Z. Visible light induced tandem reactions: an efficient one pot strategy for constructing quinazolinones using *in-situ* formed aldehydes under photocatalyst-free and room-temperature conditions. Chin Chem Lett. 2021;32(4):1427–1431.
26. Dhara K, Mandal T, Das J, Dash J. Synthesis of carbazole alkaloids by ring-closing metathesis and ring rearrangement–aromatization. Angew Chem Int Ed Engl. 2015;54(52):15831–15835.
27. Kick E, Martin R, Xie Y, Flatt B, Schweiger E, Wang T-L, Busch B, Nyman M, Gu X-H, Yan G, et al. Liver X receptor (LXR) partial agonists: biaryl pyrazoles and imidazoles displaying a preference for LXRβ. Bioorg Med Chem Lett. 2015;25(2):372–377.
28. Hu Y, Yang Y, Yu Y, Wen G, Shang N, Zhuang W, Lu D, Zhou B, Liang B, Yue X, et al. Synthesis and identification of new flavonoids targeting liver X receptor β involved pathway as

potential facilitators of Aβ clearance with reduced lipid accumulation. J Med Chem. 2013;56(15):6033–6053.
29. Nagata KO, Nakada C, Kasai RS, Kusumi A, Ueda K. ABCA1 dimer–monomer interconversion during HDL generation revealed by single-molecule imaging. Proc Natl Acad Sci U S A. 2013;110(13):5034–5039.
30. Gao J, Xu Y, Yang Y, Yang Y, Zheng Z, Jiang W, Hong B, Yan X, Si S. Identification of upregulators of human ATP-binding cassette transporter A1 via high-throughput screening of a synthetic and natural compound library. J Biomol Screen. 2008; 13(7):648–656.
31. Liu S, Sui Q, Zhao Y, Chang X. Lonicera caerulea berry polyphenols activate Sirt1, enhancing inhibition of RAW264.7 macrophage foam cell formation and promoting cholesterol efflux. J Agric Food Chem. 2019;67(25):7157–7166.
32. Kong Z, Sun D, Jiang Y, Hu Y. Design, synthesis, and evaluation of 1, 4-benzodioxan-substituted chalcones as selective and reversible inhibitors of human monoamine oxidase B. J Enzyme Inhib Med Chem. 2020;35(1):1513–1523.
33. Jia F-C, Chen T-Z, Hu X-Q. TFA/TBHP-promoted oxidative cyclisation for the construction of tetracyclic quinazolinones and rutaecarpine. Org Chem Front. 2020;7(13):1635–1639.